The hyperpolarization-activated cyclic nucleotide-gated 4 channel as a potential anti-seizure drug target

Kharouf Qays (Orcid ID: 0000-0002-0546-7238)

Cerbai Elisabetta (Orcid ID: 0000-0001-7839-1361)

Title: The hyperpolarization-activated cyclic nucleotide-gated 4 channel as a potential anti-seizure drug target

Short running title: HCN4 Channel Block Reduces Seizure Susceptibility

Authors: Qays Kharouf[1], A. Marie Phillips[1,2], Lauren E. Bleakley[1], Emma Morrisroe[1], Julia Oyrer[1], Linghan Jia[1], Andreas Ludwig[3], Liang Jin[4], Joseph A. Nicolazzo[4], Elisabetta Cerbai[5], M. Novella Romanelli[5], Steven Petrou[1] and Christopher A. Reid[1]*

Author affiliations:

1. Florey Institute of Neuroscience and Mental Health, University of Melbourne, Parkville, Victoria, Australia

2. School of Biosciences, University of Melbourne, Parkville, Victoria, Australia

3. Institut für Experimentelle und Klinische Pharmakologie und Toxikologie, Friedrich-Alexander-Universität Erlangen-Nürnberg, Erlangen, Germany

4. Drug Delivery, Disposition and Dynamics, Monash Institute of Pharmaceutical Sciences, Monash University, Parkville, Victoria, Australia

5. Department of Neurosciences, Psichology, Drug Research and Child Health, (NEUROFARBA), University of Florencevia G. Pieraccini 6I-50139 Firenze, Italy

*Corresponding author: Christopher A. Reid

Florey Institute of Neuroscience and Mental Health, University of Melbourne, Parkville 3052, Victoria, Australia Tel: +613 9035 6372 E-mail: careid@unimelb.edu.au

Word count: 3225 words (Introduction: 586, Results: 1539, Discussion and Conclusions: 1100).

Acknowledgements: This work was supported by National Health and Medical Research Council (NHMRC) Program Grant (10915693) to SP and CAR, and NHMRC Project Grant (1143101) to CAR. QK and LEB acknowledge the support of Australian Government Research Training Program Scholarships.

Conflicts of interest statement: The authors declare no conflicts of interest.

Figures: 6

Supporting information: 9 Figures and 5 tables

Author contributions: CAR conceived and organised the study. QK, AMP, and CAR designed the study. AL, EC, and MR provided materials. Data was acquired by QK, AMP, LEB, EM, JO, LJ1, LJ2, and JAN. QK, AMP, EM, LJ2, and JAN analysed data. QK, AMP, and CAR interpreted the data. The

manuscript was drafted and revised by QK, AMP, and CAR. All authors commented and discussed the manuscript.

ABSTRACT

Background and Purpose:
Hyperpolarization-activated Cyclic Nucleotide-gated (HCN) channels are encoded by four genes (*HCN1-4*) with distinct biophysical properties and functions within the brain. HCN4 channels activate slowly at robust hyperpolarizing potentials, making them more likely to be engaged during hyperexcitable neuronal network activity seen during seizures. HCN4 channels are also highly expressed in thalamic nuclei, a brain region implicated in seizure generalisation. Here we assessed the utility of targeting the HCN4 channel as an anti-seizure strategy using pharmacological and genetic approaches.

Experimental Approach:
The impact of reducing HCN4 channel function on seizure susceptibility and neuronal network excitability was studied using a HCN4 channel preferring blocker (EC18) and a conditional brain specific HCN4 knockout mouse model.

Key Results:
EC18 (10mg kg^{-1}) and brain-specific HCN4 channel knockout reduced seizure susceptibility and proconvulsant-mediated cortical spiking recorded using electrocorticography, with minimal effects on other mouse behaviours. EC18 (10μM) decreased neuronal network bursting in mouse cortical cultures. Importantly, EC18 was not protective against proconvulsant-mediated seizures in the conditional HCN4 channel knockout mouse and did not reduce bursting behaviour in AAV-HCN4 shRNA infected mouse cortical cultures.

Conclusions and Implications:
These data suggest the HCN4 channel as a potential pharmacologically relevant target for anti-seizure drugs that is likely to have a low side-effect liability in the central nervous system.

Keywords: Hyperpolarization-activated Cyclic Nucleotide-gated Channels, Ion Channels, Epilepsy, Anti-seizure, Drug Target, Neuronal Excitability.

Abbreviations: conditional HCN4 Knockout (cHCN4KO), Electrocorticography (ECoG), enhanced Yellow Fluorescent Protein (eYFP), European Data Format (EDF), Fast Fourier Transform (FFT), Hyperpolarization-activated current (I_h), Hyperpolarization-activated Cyclic Nucleotide-gated (HCN), Infrared Differential Interference Contrast (IR-DIC), Liquid Chromatography Mass Spectrometry/Mass Spectrometry (LC MS/MS), Multi-Electrode Array (MEA), Multiplicity of Infection (MOI), Quality Control (QC), Single-neuron Labelling with Inducible Cre-mediated Knockout line H (SLICK-H), Subcutaneous Pentylenetetrazole (s.c.PTZ).

Bullet point summary:

What is already known:

- HCN channels generate pacemaker activity critical for the hyper-synchronous neuronal network activity underlying seizures
- HCN4 channels are highly expressed in thalamic nuclei, a region linked to seizure generalisation

What this study adds:

- Reducing HCN4 channel function decreases seizure susceptibility and neuronal network excitability in adult mice.
- HCN4 channel block has no major impact on other measured behaviours.

Clinical significance:

- HCN4 channels are potential pharmacologically relevant targets for anti-seizure drugs with minimal adverse effects.

1 INTRODUCTION

Hyperpolarization-activated cyclic nucleotide-gated (HCN) channels are widely expressed in the brain (Biel, Wahl-Schott et al., 2009; Pape, 1996; Robinson & Siegelbaum, 2003). Four separate genes (*HCN1-4*) encode HCN channels in the central nervous system (Moosmang, Biel et al., 1999; Santoro, Chen et al., 2000). These channels carry a non-selective cation conductance, I_h, that controls fundamental neuronal functions including defining resting membrane potential, modulating the integration of dendritic synaptic input and the control of synaptic transmission, as well as controlling neuronal firing properties (Bender & Baram, 2008; Biel, Wahl-Schott et al., 2009; Nava, Dalle et al., 2014). There is a strong link between changes in HCN channel function and hyperexcitability occurring in epilepsy (Benarroch, 2013; DiFrancesco & DiFrancesco, 2015; Reid, Phillips et al., 2012) including transcriptional changes in HCN channels in both acquired and genetic rodent models of epilepsy (e.g. (Powell, Ng et al., 2008; Strauss, Kole et al., 2004)). There is also an association between neuronal hyper-excitability and genetic change in *HCN1*, *HCN2* and *HCN4* (Becker, Reid et al., 2017; Bonzanni, DiFrancesco et al., 2018; Campostrini, DiFrancesco et al., 2018; Dibbens, Reid et al., 2010; Marini, Porro et al., 2018; Nava, Dalle et al., 2014). This relationship is complex, with evidence for both increased and decreased I_h associating with heightened neuronal excitability. For example, *HCN1* and *HCN2* knockout mice both have increased seizure susceptibility (Ludwig, Budde et al., 2003; Santoro, Lee et al., 2010), while a persistent increase in I_h is observed following induced febrile seizures (Chen, Aradi et al., 2001). At a genetic level both gain- and loss-of-function *HCN1* variants, as measured in heterologous expression assays, associate with epilepsy (Marini, Porro et al., 2018; Nava, Dalle et al., 2014). Pharmacologically, the broad-spectrum I_h blockers ivabradine, caesium and ZD7288 all have anticonvulsant activity in seizure models (Kitayama, Miyata et al., 2003; Luszczki, Prystupa et al., 2013; Matsuda, Saito et al., 2008). Together, these data suggest that HCN channels, as a class, are important modulators of neuronal excitability in epilepsy.

Here we explore the role of HCN4 channels in defining neuronal network excitability in the context of epilepsy. HCN4 channels are highly expressed in the thalamus (Oyrer, Bleakley et al., 2019; Santoro,

Chen et al., 2000), a brain region implicated in seizure generalisation (Blumenfeld, 2005). HCN4 channels activate more slowly and at the most hyperpolarised potentials when compared to HCN1 and HCN2 channels (Sartiani, Mannaioni et al., 2017). This means that they are only likely to be engaged during network activity that causes robust and extended hyperpolarising episodes. Physiologically, HCN4 channels are implicated in modulating thalamic and cortical oscillations (Zobeiri, Chaudhary et al., 2019). The thalamic expression and biophysical properties of HCN4 channels position them as potential modulators of seizure activity. Consistent with this the widely used anti-epileptic drug, gabapentin, reduced the function of HCN4 channels through a left-shift in the voltage of activation (Tae, Smith et al., 2017). Increased HCN4 channel function may also be part of the mechanism underlying hyper-excitability in some forms of epilepsy with evidence including increased HCN4 mRNA levels in the pilocarpine rodent model of temporal lobe epilepsy that correlates with increased I_h in dentate granule cells (Surges, Kukley et al., 2012). Other evidence includes a switch from HCN2 to HCN4 channel expression in thalamocortical neurons in a cortical stroke model characterised by seizure development (Paz, Davidson et al., 2013). Here we show through pharmacological and molecular strategies that reducing HCN4 channel function decreases both network excitability and seizure susceptibility in adult mice, emphasizing these channels as potential targets for anti-seizure drugs.

2 METHODS

2.1 Validity of animal species or model selection

Wildtype P21 C57BL/6J mice (IMSR Cat# JAX:000664, RRID:IMSR_JAX:000664) are routinely used for testing anti-seizure drugs in proconvulsant assays (Loscher, 2011). To explore the role of HCN4 channels in defining neuronal network excitability, we developed an *in vivo* molecular approach. Global HCN4 channel knockout is embryonic lethal in mice due to its critical role in cardiogenesis (Stieber, Herrmann et al., 2003). To overcome this limitation, Herrmann and colleagues engineered an HCN4-floxed mouse that is viable and provides the opportunity to knock out HCN4 in a spatial- and/or temporal-specific manner (Herrmann, Stieber et al., 2007). In this study, we developed a double transgenic mouse model that crosses the HCN4-floxed mouse with the Tg(Thy1-Cre/ERT2,-eYFP)HGfng/PyngJ mouse line (also known as SLICK-H, IMSR Cat# JAX:012708, RRID:IMSR_JAX:012708) (Heimer-McGinn & Young, 2011) to create an inducible brain-specific knockout.

2.2 Ethical statement

All experiments were performed in accordance with the Prevention of Cruelty to Animals Act, 1986 under the guidelines of the National Health and Medical Research Council (NHMRC) Code of Practice for the Care and Use of Animals for Experimental Purposes in Australia, and were approved by the Animal Ethics Committees at the Florey Institute of Neuroscience and Mental Health and the Monash Institute of Pharmaceutical Sciences. Animal studies are reported in compliance with the ARRIVE guidelines (Kilkenny, Browne et al., 2010) and with the recommendations made by the *British Journal of Pharmacology*.

2.3 Animal welfare

Anaesthesia and analgesia were used where appropriate, as described below. Mice were monitored daily and were rapidly killed by cervical dislocation, an ANZCCART approved method.

2.4 Housing and husbandry

Animals were housed in standard 15x30x12cm cages, maintained under 12-hour dark and light cycles, and had access to dry pellet food and tap water *ad libitum*. Post-weaning P21 male C57BL/6J mice (IMSR Cat# JAX:000664, RRID:IMSR_JAX:000664) were ordered from the Animal Resources Centre (WA, Australia) or the Monash Animal Research Platform (VIC, Australia). To generate the conditional brain HCN4 knockout (cHCN4KO) mouse model, homozygous HCN4-floxed mice (Herrmann, Stieber et al., 2007) were crossed with heterozygous HCN4-floxed x hemizygous Tg(Thy1-Cre/ERT2,-eYFP)HGfng/PyngJ mice (also known as SLICK-H mice (Heimer-McGinn & Young, 2011), Jackson Laboratory (Stock No: 012708), IMSR Cat# JAX:012708, RRID:IMSR_JAX:012708). Mice were genotyped by TransnetYX (TN, USA) using PCR of DNA sourced from tails. Cre-mediated recombination was induced based on a standard Jackson laboratory protocol (Heffner, 2011). Tamoxifen (75mg kg^{-1}, i.p.) was injected for five consecutive days (P42-P46) and mice left for at least 10 days before experimentation commenced at P56 (Fig. 1A). Tamoxifen-treated SLICK-H x homozygous HCN4-floxed mice constitute our conditional HCN4 knockout (cHCN4KO) model with tamoxifen-treated SLICK-H mice forming our negative control group. For behavioural experiments involving the SLICK-H and cHCN4KO mouse models, the mix of male to female mice was approximately 50:50.

2.5 Molecular characterisation of the cHCN4KO mouse model

2.5.1 Imaging

Adult P56 SLICK-H mice (n=3) were anaesthetised via inhalation of 1-3% isoflurane and sacrificed by cervical dislocation. Brains were removed from the skulls, and coronal slices of 150µm thickness were prepared using a Vibratome. Slices were mounted in ProLong Diamond antifade reagent (Thermo Fisher, cat. no. P36962) and enclosed with no. 1.5H coverslips. Confocal image stacks were obtained using a Zeiss LSM780 system with a 20X (0.8 NA) air objective and viewed in ImageJ (ImageJ, RRID: SCR_003070, (Schneider, Rasband et al., 2012)).

2.5.2 Quantitative RT-PCR

Brains were isolated from anaesthetised mice and dissected to give hippocampus, cortex and thalamus-enriched tissue. Tissues were snap frozen in liquid nitrogen then stored at -80°C prior to being homogenized using the TRIzol method, purified using the RNeasy mini kit (Qiagen, Hilden, Germany) and assayed for quality and quantity as previously described (Phillips, Kim et al., 2014). cDNA was prepared using random primers and the transcriptor high fidelity cDNA synthesis kit (Roche Holding AG, Basel, Switzerland). Quantification was performed using a Rotor-Gene 6000 real-time PCR machine (Corbett Research, NSW, Australia). Wells were loaded with cDNA (20ng for hippocampus, 12.5ng for cortex and thalamus-enriched tissue), TaqMan Gene expression master mix (Applied Biosystems, CA, USA), and mouse specific HCN probes: HCN1 (Mm00468832_m1), HCN2 (Mm00468538_m1), and HCN4 (Mm01176086_m1). The housekeeping gene GAPDH was used for normalisation (Mm99999915_g1). All probes were labelled with a fluorescent reporter dye at the 5' end and a non-fluorescent quencher (NFQ) at the 3' end (Thermo Fisher Scientific, MA, USA). The amplification protocol consisted of two denaturing steps at 60°C (2 minutes) and 95°C (10 minutes), and 40 cycles alternating at 95°C (10s) and 60°C (60s). All RT-qPCR reactions were performed in triplicate to ensure the reliability of single values, and data analysed using Rotor-Gene 6000 series software 1.7 (Rotor-Gene 6000 series software, RRID:SCR_017552, Corbett Research, NSW, Australia). Data were analysed as previously described (Pfaffl, 2001). Results of HCN mRNA expression levels in the cHCN4KO brain (n=5 per run) are plotted relative to the mean of the SLICK-H controls (n=5 per run). This normalisation reduces sources of variation that would be present in both sample groups.

2.5.3 Western blotting

The immunoblotting procedures used comply with the recommendations made by the *British Journal of Pharmacology* (Alexander, Roberts et al., 2018) except for loading controls. Region specific brain tissue samples obtained as previously described in section 2.5.2 were homogenized in RIPA buffer (10mM Tris pH8.0, 1% Triton X-100, 0.1% sodium deoxycholate, 1% SDS, 140mM NaCl). The homogenates were then incubated with rotation for 30 minutes at 4°C, centrifuged for 20 minutes at

12,000g and supernatants retained. Sample aliquots were diluted one in 10 for quantitation by the Bradford method (Bio-Rad, CA, USA). Samples were then diluted to a final protein concentration of 5µg μL^{-1} protein, 2M urea, and 1x SDS reducing loading buffer (Laemmli, 1970), and heated for one hour at 37°C. Equal protein concentrations of control and experimental samples were separated by electrophoresis (7% and 8% poly-acrylamide SDS-PAGE) along with pre-stained Precision Plus Dual Colour Standards (Bio-Rad, CA, USA), transferred to Cellulose Nitrate, Grade SO45A3330R, (Advantec, Tokyo, Japan) and satisfactory transfer of protein by Western blotting monitored by Ponceau S (Sigma Aldrich, cat. no. P3504). Linear standard curves of control protein (25µg, 50µg, 75µg, and 100µg), were used to determine suitable protein concentrations for quantitative assessment. Filters were blocked in 0.5% skim milk, 1x TBS 1.0% and IGEPAL CA-630 (Sigma Aldrich, cat. no. I8896), 'blocker', for one hour before overnight incubation at 4°C with primary antibodies: 1:500 mouse anti-HCN4 (UC Davis/NIH NeuroMab Facility Cat# 73-150, RRID:AB_10673158), 1:500 rabbit anti-HCN2 APC-030 (Alomone Labs Cat# APC-030, RRID:AB_2313726), or 1:500 rabbit anti-HCN1 19405 (Abcam Cat# ab19405, RRID:AB_444898). The filters were washed and incubated with secondary antibodies; either goat anti-mouse polyclonal 32430 (Thermo Fisher Scientific Cat#32430, RRID:AB_1185566) 1:250, or goat anti-rabbit Poly HRP 32260 (Thermo Fisher Scientific Cat# 32260, RRID:AB_1965959) 1:15,000 for one hour at 21°C. All antibody dilutions were in 'blocker', and diluted antibodies were stored at 4°C and used a maximum of twice within a week of dilution. Western blots were analysed individually as follows: the protein signal was visualized with Clarity Western ECL Substrate (Bio-Rad, CA, USA) and the signal captured by a Bio-Rad ChemiDoc™ MP imaging system (Image Lab Software, RRID:SCR_014210) and quantified using ImageJ (ImageJ, RRID: SCR_003070, (Schneider, Rasband et al., 2012)). Exposure times varied greatly (5-400s) depending on the brain region and the HCN isoform being analysed, this was due to the differing expression levels of HCN isoforms in different regions of the brain. For each blot the data for SLICK-H control mice (n=3 or 4) were averaged, and individual values for cHCN4KO on that blot compared to this average. In order to use data from multiple blots and reduce unwanted sources of variation, these values were then plotted against their respective

controls (each control average set at a value of one). Data was not averaged across multiple blots. In a subset of Western blot experiments the number of animals was less than five and these have been described as exploratory in the supporting information (Fig. S1).

2.6 Seizure and behavioural testing

Prior to all behavioural experiments mice were acclimatized for one hour in a dimly lit behavioural room. Time to maximal hindlimb extension seizures was measured and used as the most robust seizure endpoint for all seizure assays (Chiu, Reid et al., 2008).

2.6.1 Subcutaneous pentylenetetrazole (s.c.PTZ) proconvulsant assay

Mice were injected subcutaneously with 100mg kg^{-1} PTZ and monitored for a maximum of 40 minutes for maximal hindlimb extension seizures. s.c.PTZ was injected at either 10 or 30 minutes after the injection of EC18 (10mg kg^{-1}, i.p.) or saline control.

2.6.2 Kainic acid proconvulsant assay

Mice were injected intraperitoneally with 30mg kg^{-1} kainic acid 10 minutes after the injection of EC18 (10mg kg^{-1}, i.p.) and monitored for a maximum of 60 minutes. Time to maximal hindlimb extension seizures was measured and defined as the seizure endpoint. Mice that did not have any seizures were excluded from analysis as this is likely due to poor injection of kainic acid (SLICK-H n=2, cHCN4KO n=1).

2.6.3 Thermogenic seizure assay

Mice were placed into an enclosed chamber heated to 42±1°C to induce heat-mediated clonic-tonic seizures that model febrile seizures (Reid, Kim et al., 2013). 30 minutes prior to being placed in the thermally controlled chamber mice were either injected with EC18 (10mg kg^{-1}, i.p.) or saline control. Mice were culled by cervical dislocation immediately after the first observed seizure, or 20 minutes after being placed in the chamber if they remained seizure-free in line with ethics requirements.

2.6.4 Open field exploratory locomotion assay

Mice were individually placed in a square mouse open field 27.3x27.3x20.3cm arena (Med Associates Inc., St. Albans, VT) and allowed to move freely for one hour. Recorded data indicating distance

travelled and resting duration was then compiled using locomotion analysis software (MED Associates Activity Monitor software, RRID:SCR_014296, Med Associates Inc., Vermont, USA).

2.6.5 Light/dark transition test

A square mouse open field arena was divided into two equal 27.3x13.7cm light and dark zones using a black acrylic box insert with a small opening. The light zone was illuminated at 750lx. Mice were individually placed inside the dark zone at the start of the test and allowed to freely explore both zones for 10 minutes. Recorded data indicating the number of entries and duration spent in each zone was compiled using locomotion analysis software (MED Associates Activity Monitor software, RRID:SCR_014296, Med Associates Inc., Vermont, USA).

2.6.6 Elevated plus maze

The elevated plus maze was raised 40cm from the floor and consisted of two open arms and two enclosed arms with 55cm high walls extending from the centre. Mice were individually placed in one of the enclosed arms and allowed to freely roam the maze for 10 minutes while being recorded by a ceiling-mounted video camera. Entries into each arm along with their respective durations were measured using tracking software (EthoVision XT, RRID:SCR_000441, Noldus, Wageningen, Netherlands).

2.6.7 Grip strength

Mouse limb neuromuscular strength was assessed using a grip strength isometric force transducer (Bioseb, Chaville, France) connected to a 10x10cm wire grid. Mice were placed on the wire grid and gently pulled backwards by their tails until they released. The peak force applied by the mouse's limbs was recorded for three separate trials to ensure the reliability of each trial. The maximal force applied by each mouse over the three trials was used for statistical analysis.

2.7 Pharmacokinetic studies

2.7.1 Intraperitoneal administration of EC18 to C57BL/6J mice

On the day of experiments, EC18 was freshly dissolved in saline and a 200µL solution equivalent to 10mg kg^{-1} was administered into the lower abdominal quadrant of male C57BL/6J mice (IMSR Cat#

JAX:000664, RRID:IMSR_JAX:000664). Blood and brain samples were collected at 10, 20, 30 and 60 minutes following the initial dosing. Concentrations of EC18 in plasma and brain homogenate were measured using LC MS/MS assay. To more accurately determine the brain concentration of EC18, the concentration of EC18 remaining within the brain microvasculature was subtracted from the brain homogenate concentration using the mouse brain microvascular volume of 0.017mL g^{-1} (Nicolazzo, Steuten et al., 2010).

2.7.2 Preparation of calibration standards and mouse samples

A stock of EC18 (10mg mL^{-1}) was first prepared in MilliQ water. For plasma samples, working standard solutions with concentrations of 0.5, 1, 2, 5 and 10µg mL^{-1} were prepared by serial dilution of the stock solution in MilliQ water. The low- and high-quality control (QC) solutions of 0.5 and 10µg mL^{-1} were prepared in the same manner using an independently prepared stock solution. Calibration and QC samples were prepared by spiking 10µL of the working solutions into 90µL of blank plasma obtained from C57BL/6J mice (IMSR Cat# JAX:000664, RRID:IMSR_JAX:000664). The mixture was then vortexed for 5s. Plasma samples were prepared in the same manner, except that 10µL of MilliQ water was added into 90µL of plasma sample instead of the working solution. To each mixture, 0.5mL of ethyl acetate was added, followed by vortex mixing for 20 minutes at room temperature and centrifugation for five minutes at 1,000g. The supernatant was then collected and dried with nitrogen gas. The residue was reconstituted in 100µL of MilliQ water and analysed by the LC MS/MS method described in the following section. To measure the concentration of EC18 in brain samples, working standard solutions with concentrations of 0.1, 0.5, 1, 5 and 10µg mL^{-1} were prepared by serial dilution of stock solution (10mg mL^{-1}) in MilliQ water. The low and high QC solutions of 0.1 and 10µg mL^{-1} were prepared in the same manner using an independently prepared stock solution. Calibration and QC samples were prepared by spiking 30µL of the working solutions into 270µL of blank brain homogenate to achieve concentrations of 30, 150, 300, 600, 1,500 and 3,000ng g^{-1}. The mixture was then vortexed for 5s. Brain homogenate samples were prepared in the same manner, except that 30µL of MilliQ water was added into 270µL of brain homogenate sample instead of the

working solution. To each mixture, 1.5mL of ethyl acetate was added, followed by vortex mixing for 20 minutes at room temperature and centrifugation for five minutes at 1,000g. The supernatant was then collected and dried with nitrogen gas. The residue was reconstituted in 100µL of MilliQ water and analysed by the LC MS/MS method described in the following section. Each of the four QC samples at each concentration was measured and compared to determine the intraday assay precision and accuracy. Precision was expressed as relative standard deviation (%) and accuracy was calculated as the difference between the measured and nominal concentration expressed as percentage (Table S1).

2.7.3 LC MS/MS analysis

An Ascentis® Express C_{18} column (2.7µm particle size, 2.1x50mm internal diameter) with a Phenomenex Security Guard™ C_{18} guard column (2.0x4.0mm) was used for the measurement of EC18. Samples of 10µL were injected into a Shimadzu HPLC system consisting of two LC-30AD pumps; a SIL-30AC autoinjector and a DGU-20A_5 degasser (Shimadzu, Kyoto, Japan). Mobile phase A and B were 0.1% (v/v) formic acid in MilliQ water and methanol, respectively. The gradient profile developed to determine the concentration of EC18 was: 0-1 minutes, 90% A; 1-1.5 minutes, 75% A; 1.5-2 minutes, 75% A; 2-2.5 minutes, 50% A; 2.5-3.5 minutes, 50% A; 3.5-4 minutes, 90% A. A Shimadzu LC MS/MS-8050 triple quadrupole mass spectrometer (Shimadzu, Kyoto, Japan) was used to perform the mass spectrometry in the electrospray ionization positive mode by multiple reaction monitoring (*m/z* 533.10 to 258.25). Nitrogen was used as the nebulizing gas and drying gas, and the temperatures of the desolvation line and heat block were set at 250°C and 400°C, respectively. The dwell time was set at 100ms.

2.8 Electrocorticography (ECoG) monitoring

2.8.1 ECoG electrode implantation

ECoG electrode implantation was performed at P26-30 on male C57BL/6J mice (n=13) (IMSR Cat# JAX:000664, RRID:IMSR_JAX:000664), and at P52-60 on SLICK-H (n=8) and cHCN4KO (n=10) mice. Mice were weighed then anaesthetised via inhalation of 1-3% isoflurane and placed on a stereotaxic frame. Three holes, each 1mm in diameter, were drilled to secure stainless-steel skull screws that act as

epidural ECoG electrodes. Two screws were placed bilaterally over the somatosensory (S1) cortex and used as the active channel electrodes (±3.0mm lateral to the midline, -1.0mm caudal to bregma). The third screw was placed immediately caudal to the lambdoid suture 0.5mm lateral from the midline towards the right side of the skull and used as the reference channel electrode. A ground electrode made of silver wire was affixed to the skull immediately caudal to the lambdoid suture 0.5mm lateral from the midline towards the left side of the skull. The reference, ground and two active channel electrodes were connected to a mouse EEG head mount (8201-EEG Pinnacle technology Inc., KS, USA) via silver leads (Cat No. 785500, A-M Systems Inc., WA, USA). Self-curing acrylic resin (Vertex-Dental B.V., Soesterberg, Netherlands) was used to hold the head mount and skull screws in place. Lidocaine hydrochloride (2%, s.c., Ilium, NSW, Australia) was injected subcutaneously prior to surgical incision to provide local anaesthesia to the scalp. Meloxicam (1mg kg^{-1}, i.p., Ilium, NSW, Australia) was given as an analgesic and mice were left to recover for 72 hours before experimentation.

2.8.2 ECoG recording of low-dose PTZ-induced spiking

Mice were independently housed during recordings in a clear 30x15x15cm plexiglass container. Prior to recording, the head mount was linked to a mouse preamplifier (8406-SE, Pinnacle Technology Inc.) and connected to a 4-channel data conditioning/acquisition system (8200-K1-SE3, Pinnacle Technology Inc.). Data was acquired at 2,000Hz and filtered (40Hz low-pass and 0.5Hz high-pass) using Sirenia Acquisition 1.7.5 software (Sirenia Acquisition, RRID:SCR_016183, Pinnacle Technology Inc.). For C57BL/6J mice (IMSR Cat# JAX:000664, RRID:IMSR_JAX:000664), each recording consisted of a 30 minute baseline measurement followed by an injection of EC18 (10mg kg^{-1}, i.p.). 10 minutes post administration of EC18, male C57BL/6J mice were injected with PTZ (60mg kg^{-1}, s.c.) to induce spiking and recorded for an additional 30 minutes. For SLICK-H and cHCN4KO mouse recordings, PTZ was injected immediately after the 30 minute baseline recording to induce spiking and recorded for an additional 30 minutes. Mice were then culled by cervical dislocation within 30 minutes of administration of PTZ.

2.8.3 ECoG signal analysis

Recordings were converted to the European data format (EDF) then imported into LabChart Reader software 8.1 (LabChart Reader software, RRID:SCR_017551, ADInstruments, NSW, Australia). Five minute power spectrograms were produced by running a Fast Fourier Transform (FFT) algorithm with a Cosine-Bell data window. The window size was 1,024 data points with an overlap of 87.5%. Results are plotted as heatmaps with power expressed as μV^2.

2.8.4 Quantification of PTZ-induced spikes

Spikes were detected and quantified using automated simple threshold cyclic measurements. Spike detection thresholds ranging between 200-300µV were set manually per mouse based on relative baseline and spiking amplitudes. The rate of PTZ-induced spikes detected per minute is calculated for a maximum of the first 10 minutes post PTZ administration or to the time that a seizure occurred.

2.9 Primary neuronal culture

2.9.1 Culture preparation

Cells were dissociated from cortices of P0-P2 C57BL/6J mice (IMSR Cat# JAX:000664, RRID:IMSR_JAX:000664) (n=8-10), pooled to give an evenly mixed population and cultured on polyethyleneimine/laminin-coated 24-well multielectrode array plates (Multichannel Systems, Reutlingen, Germany) or for cDNA analysis in coated 6-well plates, as previously described (Gazina, Morrisroe et al., 2018; McSweeney, Gussow et al., 2016). Cells were plated at a density of $2x10^6$ per well in the 6-well plates and 375,000 per well in the 24-well MEA plate in culture medium as described (Gazina, Morrisroe et al., 2018). At day three *in vitro*, cytosine arabinoside (5µM, Merck KGaA, Darmstadt, Germany) was added to the medium to inhibit glial proliferation and removed 48 hours later. Medium was replaced every two days subsequently.

2.9.2 shRNA Design and virus production

HCN4 shRNA vectors were designed by Vector Biolabs (Malvern, PA, USA). U6 promotor driven shRNA screening was completed on five clones. shRNA sequence CCGGCTCCAAACTGCCGTCTAATTTCTCGAGAAATTAGACGGCAGTTTGGAGTTTTTG (MISSION® TRC

shRNA TRCN0000252673), was shown to reduce mouse HCN4 transcript by ~83% and was used for viral production. AAV(1/2)-GFP-U6-mHCN4-shRNA (AAV-HCN4 shRNA, $3.4x10^{13}$ GC mL^{-1}) was engineered and included the shRNA sequence driven under a U6 promotor and GFP under a CMV promotor. A standard AAV(1/2)-GFP-U6-scrmb-shRNA (AAV-control, $7.1x10^{13}$ GC mL^{-1}) was used as a negative control.

2.9.3 Viral infection and validation

The cortical cultures were left to mature for 12 days before addition of either AAV-HCN4 shRNA or AAV-control at a multiplicity of infection (MOI) of 15,000 per plated cell. Cells were monitored for GFP fluorescence from six days post transfection. Expression was visible in both cultures at seven days post transfection.

2.9.4 Immunocytochemistry

Cells were cultured as previously described in section 2.9.1 and grown for 10 days post viral infection in an 8-well Nunc™ Lab-Tek™ Chamber Slide System (Thermo Fisher, cat. no. 177402PK) for immunocytochemistry. Cells were fixed in 4% paraformaldehyde in 0.1M phosphate buffer pH7.4 (PB) for 10 minutes at room temperature (RT), permeabilised in 0.3% Triton X-100 in PB for six minutes, and then blocked in 1% FBS/22.52mg ml^{-1} glycine in PB containing 0.1% Tween20 for 30 minutes at RT. Cells were washed three times with PB between each procedure. Blocked cells were incubated at 4°C for 16 hours with primary antibodies: 1:500 Guinea Pig anti-NeuN (Sigma Aldrich, Millipore Cat# ABN90P, RRID: AB_2341095) and 1:500 Chicken anti-GFP (Abcam Cat# ab13910, RRID: AB_300798). Cells were washed in PB and incubated with secondary antibodies: 1:1,000 CF®594 Donkey anti-Guinea Pig (Biotium Cat# 20170-1, RRID: AB_10854394) and 1:10,000 Goat anti-Chicken Alexa Fluor® 488 (Molecular Probes Cat# A-11039, RRID: AB_142924) for one hour at RT. After washing with PB the wells were removed from the chamber base and the slide mounted in ProLong Diamond antifade reagent (Thermo Fisher, cat. no. P36962) and enclosed with no. 1.5H coverslips. Confocal images were obtained using a Zeiss LSM780 system with a 20X (0.8 NA) air objective and viewed in ImageJ (ImageJ, RRID: SCR_003070, (Schneider, Rasband et al., 2012)).

2.9.5 Analysis of viral knockdown of HCN expression

Cells were cultured for 14 days post transfection before harvesting. Three independent experiments were conducted, each involving pooled cells from 8-10 neonates. Cells were harvested by scraping from the 6-well plates and pelleted by centrifugation. Total RNA was prepared by the TRIzol method, purified using the RNeasy mini kit (Qiagen, Hilden, Germany) and assayed for quality and quantity as previously described (Phillips, Kim et al., 2014). cDNA was prepared using random primers and the high-fidelity cDNA Synthesis Kit (Roche Holding AG, Basel, Switzerland). qPCR was carried out on 10µg cDNA samples, in triplicate to ensure the reliability of single values, using hydrolysis probes HCN1 (Mm00468832_m1), HCN2 (Mm00468538_m1), HCN4 (Mm01176086_m1) and GAPDH (Mm99999915_g1). Results were analysed as described previously (Phillips, Kim et al., 2014).

2.9.6 Multi-Electrode array (MEA) data acquisition

10 days post viral transfection, two 24-well MEA plates, each containing 12 wells of AAV-HCN4 shRNA or AAV-control transfected cortical cells, were analysed on a Multiwell-MEA headstage (Multichannel Systems, Reutlingen, Germany). The plates were placed in a temperature and CO_2 controlled enclosed recording system and allowed to equilibrate for five minutes prior to baseline data collection for six minutes at a rate of 20,000Hz. Data acquisition was carried out using the Multiwell Screen software (Multichannel Systems), and signals were filtered as previously described (Gazina, Morrisroe et al., 2018). The plates were then removed from the headstage and 250µl of medium (50% of the total medium) was replaced with 250µl of pre-warmed medium containing 5µl of 1mM EC18 or water (vehicle). The plates were returned to the incubator for two hours prior to re-analysis as per the method described above.

2.9.7 MEA feature extraction and analysis

Voltage signals were high-pass filtered at 300Hz and spikes detected with custom MATLAB scripts that used a criterion of peak amplitude greater than six times the standard deviation of noise. Noise levels were calculated in 20s blocks. Bursts in single channels (single–channel bursts) and network bursts were detected using an adaptive algorithm based on firing rates as described previously (Mendis,

Morrisroe et al., 2016). Bursts on single channels were defined as rapid successions of three or more spikes while network bursts were defined as events in which more than 20% of single-channel bursts overlapped in time. For EC18 experiments, means +/- SEM (n=11-12) are presented as the percentage change relative to baseline, to reduce unwanted variation between wells as previously described (Mendis, Berecki et al., 2019).

2.10 Pharmaceutical materials

Tamoxifen (Sigma Aldrich, cat. no. T5648) was freshly dissolved in corn oil (Sigma Aldrich, cat. no. C8267) by shaking at 60rpm overnight at 37°C. Pentylenetetrazole (Sigma Aldrich, cat. no. P6500) and kainic acid monohydrate (Sigma Aldrich, cat. no. K0250) were dissolved in normal saline to prepare an injectable solution at concentrations of 200mg mL^{-1} and 3mg mL^{-1} respectively. The HCN4 channel preferring blocker EC18 (Prof Romanelli, Florence, Italy) was dissolved in MilliQ water to make a 10mg mL^{-1} stock solution and further diluted in normal saline to 1mg mL^{-1} for injection.

2.11 Group size

We set the group size as the number of independent values in each experiment. For MEA experiments this was the number of independent wells used. The number of animals and independent wells used in each experiment was predetermined based on analyses of similar published works (Chiu, Reid et al., 2008; Mendis, Morrisroe et al., 2016; Reid, Kim et al., 2013). Statistical analysis was undertaken only for experiments where each group size was at least five ($n \geq 5$).

2.12 Randomization

For experiments investigating the impact of brain-specific HCN4 knockout on PTZ-induced seizure susceptibility equal numbers of the SLICK-H and cHCN4KO mice were chosen based on genotype. The boxes were then deidentified and assigned a random number. Mice were then selected for injection randomly from a maximum of three mice in any given box. Mice numbers were decoded by an independent researcher after experimentation. For other experiments no formal method was used to generate a randomisation sequence for animals used. For EC18 experiments, male C57BL/6J mice

were pulled from the combined cohort sequentially with alternate mice receiving either drug or vehicle control.

2.13 Blinding

Different researchers were involved while conducting seizure and behavioural experiments with the operators being blinded to the treatment.

2.14 Data and analysis

For all *in vivo* experiments involving EC18, only male mice were used to minimise possible variation between sexes. All other experiments included both male and female mice to minimize the number of litters used in line with ethical considerations. Statistical significance of Kaplan–Meier curves was determined using a log-rank (Mantel-Cox) test. Analyses where comparisons were relative to wildtype or control, including Quantitative RT-PCR, Western blot and MEA data used the Wilcoxon signed-rank test. The Shapiro-Wilk test was used to establish if data had a normal distribution prior to other statistical analysis. F-tests were used routinely to establish if differences in variance existed between groups. If F-tests showed a significant difference in variance between groups, a nonparametric two-tailed Mann-Whitney U test was used. A two factor ANOVA test was used to determine sex differences in behavioural assays. All other statistical comparisons were based on Student's two-tailed unpaired t-test. GraphPad Prism 7 was used as the statistical analysis software (GraphPad Prism, RRID:SCR_002798, CA, USA). Unless stated otherwise, all data are presented as mean and error bars indicate the standard error of the mean (SEM). Statistical significance was set at $p<0.05$. Except where stated, the data and statistical analysis complies with the recommendations on experimental design and analysis in pharmacology (Curtis, Alexander et al., 2018).

2.15 Nomenclature of Targets and Ligands

Key protein targets and ligands in this article are hyperlinked to corresponding entries in http://www.guidetopharmacology.org, the common portal for data from the IUPHAR/BPS Guide to PHARMACOLOGY (Harding et al., 2018), and are permanently archived in the Concise Guide to PHARMACOLOGY 2019/20 (Alexander et al., 2019).

3 RESULTS

3.1 Validation of HCN4 Channel Knockout in an Adult Mouse Model

We generated a double transgenic mouse model by crossing the HCN4-floxed mouse with the Tg(Thy1-Cre/ERT2,-eYFP)HGfng/PyngJ mouse line (also known as SLICK-H) (Heimer-McGinn & Young, 2011) (Fig. 1A). This conditional line has a tamoxifen-inducible Cre-mediated recombination system driven by the Thy1 promoter (Heimer-McGinn & Young, 2011). We have chosen this mouse model as the Thy1 promoter expresses Cre recombinase widely in the CNS, but expression is absent in cardiac tissue. The inducible nature of this mouse line allows us to test the impact of HCN4 knockout without developmental confounds. eYFP is driven independently as a marker of cells in which recombination should occur in the SLICK-H mouse (Fig. 1A+B). In the HCN4 floxed mouse, exon 4 of *HCN4* is flanked by loxP sites and deleted using the Cre/loxP system (Fig. 1A). Tamoxifen (75mg kg^{-1}, i.p.) was injected for five consecutive days (P42-P46) and mice left for at least 10 days before experimentation commenced (Fig. 1A). Tamoxifen-treated hemizygous SLICK-H x homozygous HCN4-floxed mice constitute our conditional HCN4 knockout (cHCN4KO) model with tamoxifen-treated hemizygous SLICK-H mice forming our negative control group.

The conditional knockout of brain HCN4 channels had no significant effect on the weight of the mice (Fig. 1C). We used quantitative RT-qPCR and Western blot analysis to explore the extent of reduction in HCN4 channel expression in thalamus, cortex and hippocampus tissue of cHCN4KO mice. HCN4 mRNA levels were reduced significantly in all tissues of the cHCN4KO mouse compared to the SLICK-H controls (Fig. 1D+S2). The expression of HCN1 and HCN2 mRNA in cortex and thalamus-enriched tissue was unchanged (Fig. 1D). Western blot analysis confirmed a significant reduction in HCN4 channel protein in cortex (n=7) and thalamus-enriched tissue (n=6) of cHCN4KO mice (Fig. 1E+F). A similar reduction of HCN4 protein expression was seen in an exploratory Western blot on hippocampal tissue (Fig. S1). Exploratory Western blots of HCN1 and HCN2 isoforms showed similar levels in cHCN4KO and SLICK-H in hippocampal tissues (Fig. S1). SLICK-H HCN1 protein levels in thalamus-enriched tissue were too low for ImageJ density scans, likely due to the low expression of this isoform in this brain

region (Fig. 1F) (Santoro, Chen et al., 2000). Typical uncropped Western blots are shown in the supporting information (Fig. S3-7).

3.2 Neuronal Excitability and Seizure Susceptibility is Reduced in the cHCN4KO Mouse Model

We next investigated the seizure susceptibility of the cHCN4KO model using two standard proconvulsant tests: susceptibility to subcutaneous pentylenetetrazole and response to kainic acid. cHCN4KO mice were significantly less susceptible to s.c.PTZ (100mg kg^{-1}) with an increase in latency to hindlimb extension relative to the SLICK-H control (Fig. 2A, Table S2). Also, cHCN4KO mice were significantly less susceptible to kainic acid (30mg kg^{-1}, i.p.) with an increase in latency to hindlimb extension relative to the SLICK-H control (Fig. 2B, Table S2).

To directly test the impact of HCN4 knockout on brain excitability, electrocorticography (ECoG) recordings were made following the injection of low-dose PTZ (60mg kg^{-1}, s.c.) (Fig. 2C). Sustained spiking on ECoG was evident within minutes of PTZ injection in both the cHCN4KO and SLICK-H control mice (Fig. 2C+D). However, cHCN4KO mice displayed significantly less spiking than SLICK-H control mice consistent with a reduction in proconvulsant-induced excitability (Fig. 2C-E). These data strongly support the premise that HCN4 channels are important arbiters of neuronal network excitability and modulate seizure susceptibility.

3.3 Subtle Behavioural Phenotype in the cHCN4KO Mouse Model

The cHCN4KO mice performed at close to SLICK-H control mice levels in a set of behavioural tests. cHCN4KO mice showed a reduction in distance travelled and an increase in resting duration early in the locomotion test when compared to the SLICK-H control mice (Fig. 3A+C). This normalised with time and there was no significant difference in the overall distance travelled or resting duration (Fig. 3B+D). The grip strength of cHCN4KO mice was significantly greater than the SLICK-H mice (Fig. 3E), but there was no difference on the elevated plus maze (Fig. 3F+G) or in performance on the rotarod (Fig. 3H). cHCN4KO mice did show a significant increase in the number of light zone entries in the light/dark transition test, although the duration spent in the light zone was not different relative to the SLICK-H control mice (Fig. 3I+J). Additional parameters extracted from the behavioural tests are

presented in Table S3. These data suggest that a reduction in neuronal HCN4 channel expression can protect mice from proconvulsant seizures with no major impact on other measured behaviours.

3.4 The HCN4 Preferring Compound EC18 Reduces Seizure Susceptibility

EC18, a structural derivative of the bradycardic drug zatebradine, blocks recombinant HCN4 channels with approximately six-fold increased sensitivity over HCN1 and HCN2 channels (Del Lungo, Melchiorre et al., 2012; Romanelli, Del Lungo et al., 2019; Romanelli, Sartiani et al., 2016). We first established the pharmacokinetic profile of EC18 in the C57BL/6J mouse strain. A liquid chromatography mass spectrometry/mass spectrometry (LC MS/MS) was developed, allowing the measurement of EC18 levels in plasma and brain samples. There was a rapid increase in EC18 plasma levels following an injection of EC18 (10mg kg^{-1}, i.p.), peaking at 10 minutes and reducing to low levels within one hour (Fig. 4A). Brain homogenate levels were lower and peaked at 20 minutes before rapidly declining (Fig. 4A). This data provided a time profile on which to design our testing of EC18 in proconvulsant seizure tests. Wildtype male P40 mice were injected with EC18 (10mg kg^{-1}, i.p.), and after 10 minutes their seizure susceptibility was tested using the s.c.PTZ proconvulsant assay (Fig. 4B). Mice injected with EC18 showed significantly longer latency to hindlimb extension than those injected with saline (Fig. 4B, Table S4). A separate cohort of male mice was left for 30 minutes following injection, a time point where EC18 levels in the blood and brain have dropped significantly (Fig. 4C). Mice injected with EC18 at this later time point also showed a significantly longer latency to hindlimb extension (Fig. 4C, Table S4). Although it is difficult to make direct comparisons due to cohort-to-cohort differences in controls, the seizure protection of EC18 at this later time point appeared to be decreased, consistent with the reduced brain and plasma levels. In another experiment, EC18 (10mg kg^{-1}, i.p.) was injected 30 minutes prior to placing wildtype P21 male mice in a heated chamber that models febrile seizure syndromes (Reid, Kim et al., 2013). EC18 delayed the development of heat-mediated clonic-tonic seizures (Table S4). Importantly, EC18 (10mg kg^{-1}, i.p.) was not effective in reducing seizure susceptibility in the cHCN4KO mouse (Fig. 4D, Table S5) but was effective in the SLICK-H control (Table S5). We also tested the impact of EC18 on the rate of low-dose PTZ-induced cortical

spiking recorded with ECoG. EC18 (10mg kg^{-1}, i.p.) significantly reduced ECoG cortical spiking in wildtype mice (Fig. 4E-G), consistent with a dampening of cortical excitability.

3.5 The HCN4 Channel Preferring Blocker EC18 has Minimal Impact on Locomotion

Behaviourally, EC18 (10mg kg^{-1}, i.p.) injected at 30 minutes prior to testing caused an initial reduction in locomotion (Fig. 5A) but no difference was observed in overall distance travelled (Fig. 5B), nor was there a change in resting duration (Fig. 5C+D).

3.6 EC18 Reduces Firing and Network Burst Activity through HCN4 Channels in Cortical Cultures

Having established that EC18 shows seizure protective properties in mice we next tested its impact on neuronal network behaviour. We developed a culture-based assay in which HCN4 expression was reduced using a shRNA knock-down approach. Cortical neuronal cultures were infected using AAV1/2-HCN4 shRNA (AAV-HCN4 shRNA) or AAV1/2-scrambled shRNA that acted as a control (AAV-control). GFP expression in the cortical cultures was robust for both viruses and colocalised with the neuronal marker, NeuN (Fig. 6A-F). A wide field view of these cortical cultures is shown in the supporting information (Fig. S8). Quantitative RT-qPCR confirmed that HCN4 mRNA is reduced by ~70% in AAV-HCN4 shRNA relative to AAV-control treated cells (Fig. 6G). However, HCN1 mRNA levels were significantly increased, as were HCN2 mRNA levels although to a lesser extent (Fig. 6G). Neuronal network activity was measured in 24-well multi-electrode array (MEA) plates. Raster plots of firing patterns were generated to allow quantification of network activity (Fig. S9). Mean firing rate and network burst rate are measures that are known to be reduced by the commonly used anti-epileptic drugs carbamazepine and sodium valproate (Colombi, Mahajani et al., 2013). In AAV-control cultures, EC18 reduced the mean firing rate and reduced network burst rate (Fig. 6H+I) consistent with a reduction in network excitability (Colombi, Mahajani et al., 2013). Importantly, in AAV-HCN4 shRNA infected cultures EC18 had minimal impact on mean firing rate or network burst rate (Fig. 6H+I). Furthermore, EC18 also increased the burst duration in AAV-control infected cultures (1.19 ± 0.04), an effect that was not seen in AAV-HCN4 shRNA infected cultures (1.00 ± 0.1). It is important to note that the interpretation of how molecular HCN4 channel knock-down directly modulates neuronal networks

in this culture assay is confounded by compensatory changes in HCN1 and HCN2 mRNA levels. Although we cannot exclude that the lack of effect of EC18 is due to a change in the 'state' of the network, our data is consistent with the idea that EC18 is acting through the HCN4 channel to modulate neuronal network excitability.

4 DISCUSSION AND CONCLUSIONS

Here we provide evidence that HCN4 channels are important arbiters of neuronal network excitability. The conditional brain knockout of HCN4 channels in adult mice reduced seizure susceptibility in proconvulsant assays, and also reduced low dose PTZ-induced spiking recorded with ECoG. Only minor behavioural changes were observed in the cHCN4KO mouse, consistent with those observed in the Nestin-cre conditional HCN4 channel knockout mouse (Zobeiri, Chaudhary et al., 2019). We also demonstrate that the preferentially selective HCN4 channel blocker, EC18, reduced proconvulsant-mediated seizure susceptibility and reduced PTZ-induced ECoG spiking in male wildtype mice. The anti-seizure effect of EC18 was occluded in the cHCN4KO mouse. Furthermore, EC18 did not reduce the firing rate or bursting in cortical cultures treated with AAV-HCN4 shRNA. We used established rodent proconvulsant models that can predict human efficacy and are considered useful tools for screening compounds in early stages of drug discovery (Loscher, 2011; Yuen & Troconiz, 2015). However, testing EC18 on other acquired and genetic models of epilepsy will be important. Importantly, the sex-specific impact of pharmacological and molecular 'block' of HCN4 channels on seizure susceptibility has not been systematically studied here and requires further investigation. Overall, these data support the notion that HCN4 channels are important arbiters of brain excitability and that blockers of these channels may be effective anti-seizure drugs.

EC18 is a compound that has approximately six-fold increased selectivity for HCN4 over HCN1 and HCN2 isoforms based on heterologous expressed channels (Del Lungo, Melchiorre et al., 2012; Romanelli, Del Lungo et al., 2019; Romanelli, Sartiani et al., 2016). The selectivity found in recombinant systems is maintained in tissues expressing different HCN isoforms. EC18 blocked I_h in guinea pig sinoatrial cells and dog cardiac Purkinje fibres that express HCN4 channels, while having minimal impact in dorsal root ganglia neurons that express HCN1 as the major isoform (Del Lungo, Melchiorre et al., 2012). Within the central nervous system, EC18 blocks I_h on thalamic neurons with an EC_{50} of about 10μM (Romanelli, Del Lungo et al., 2019). EC18 also weakly blocks slow delayed rectifier K^+ channels at 10μM (Romanelli, Del Lungo et al., 2019). In neuronal cultures, the reduction in both mean

firing and network burst rates was occluded by knocking down HCN4 mRNA using an shRNA strategy. This evidence indicates that EC18 is acting primarily through HCN4 channels to reduce network excitability and consequently seizure susceptibility.

HCN4 expression is limited in the CNS with highest levels seen in the thalamus, medial habenula and olfactory bulb (Santoro, Chen et al., 2000). The thalamus is well positioned to contribute to seizure generalisation. Thalamic relay neurons in particular are thought to be a key requirement for the propagation of generalised seizures (Blumenfeld, 2005). Thalamic relay neurons from a genetic rodent model of generalised seizures have increased I_h, implicating changes in this current as part of the pathogenic process (Cain, Tyson et al., 2015). Furthermore, in their genetic rodent model, David and colleagues demonstrated that direct broad-spectrum pharmacological block of HCN channels in the thalamus decreased thalamocortical neuron firing and abolished spontaneous seizures (David, Carcak et al., 2018). Molecular knockdown of HCN2 channels, also highly expressed in the thalamus, similarly reduced seizures. This is in contrast with other studies that indicate that reductions in HCN2 channel activity in thalamocortical neurons induce generalised seizures (Chung, Shin et al., 2009; Hammelmann, Stieglitz et al., 2019; Ludwig, Budde et al., 2003). Interestingly, while specific HCN2 channel knockout in the ventrobasal nuclei was sufficient to induce generalised seizures, HCN4 channel knockout was without effect (Hammelmann, Stieglitz et al., 2019). This suggests that HCN2 and HCN4 subunits play distinct roles within thalamic neurons and that targeting each independently may produce different outcomes on excitability. Zobeiri and colleagues have recently demonstrated that brain-specific HCN4 channel knockout reduces thalamocortical neuron rebound burst firing and network bursting behaviour in brain slice preparations (Zobeiri, Chaudhary et al., 2019). The cellular changes observed in the HCN4 KO mouse are associated with a slowing of thalamic and cortical oscillations in awake mice (Zobeiri, Chaudhary et al., 2019) providing a plausible cellular basis for seizure protection. Therefore, our hypothesis is that HCN4 inhibition reduces thalamocortical bursting behaviour and consequently reduces the propagation of seizures although confirming this will require additional study.

HCN4 channel blockers are likely to be well tolerated. HCN4 channels are highly expressed in cardiac tissue, especially in the sinoatrial node, making them important regulators of heart rate (Herrmann, Hofmann et al., 2012). The broad-spectrum HCN channel blocker, ivabradine, causes bradycardia and is used clinically for the treatment of angina pectoris and systolic heart failure (Koruth, Lala et al., 2017). Importantly, ivabradine has a very favourable safety profile with bradycardia and self-limiting visual disturbances as side-effects (Koruth, Lala et al., 2017). Therefore, systemic HCN4 channel blockers are expected to have, at worst, a similar favourable peripheral side-effect profile to ivabradine. It is difficult to draw conclusions about potential central nervous system side effects as ivabradine does not cross the blood brain barrier well (Savelieva & Camm, 2006; Savelieva & Camm, 2008). However, in mice, EC18 had minimal side-effects, showing only a reduction in locomotion at early time points. Furthermore, seizure protection in the cHCN4KO mouse also occurred in the context of minimal behavioural changes. These data suggest that both peripheral and central side effects of selective HCN4 channel blockers are likely to be minimal.

Efforts to develop more selective HCN4 blockers are warranted. EC18 has provided a good proof-of-concept small molecule for testing the impact of HCN4 channels on neuronal excitability. However, EC18 only has partial selectivity for HCN4 channels (Del Lungo, Melchiorre et al., 2012; Romanelli, Del Lungo et al., 2019; Romanelli, Sartiani et al., 2016). Therefore, despite demonstrating that the anti-bursting and anti-seizure impact of EC18 is occluded when HCN4 channels are knocked down, we cannot exclude that EC18 is not having these effects through actions on HCN1 and/or HCN2 channels. Moreover, poor brain penetration and rapid elimination from brain and plasma make EC18 a less than ideal therapeutic drug. Small molecules with improved pharmacokinetics and selectivity are needed. Gabapentin causes a shift of the voltage of activation, which is selective for HCN4 over HCN1 and HCN2, arguing that absolute HCN subunit selectivity may be possible (Tae, Smith et al., 2017). Development of strategies geared at reducing HCN4 protein through molecular methods may also be worth pursuing. These could include the development of viral tools that deliver shRNA, or antisense oligonucleotides designed to specifically knock down the HCN4 protein.

In conclusion, we provide strong evidence that HCN4 channels modulate neuronal excitability and seizure susceptibility. We also propose that HCN4 channels may be pharmacologically relevant targets for anti-seizure drugs.

DECLARATION OF TRANSPARENCY AND SCIENTIFIC RIGOUR

This Declaration acknowledges that this paper adheres to the principles for transparent reporting and scientific rigour of preclinical research as stated in the BJP guidelines for Design & Analysis, Immunoblotting and Immunochemistry, and Animal Experimentation, and as recommended by funding agencies, publishers and other organisations engaged with supporting research.

REFERENCES

Alexander, S. P. H., Mathie, A., Peters, J. A., Veale, E. L., Striessnig, J., Kelly, E., . . . Collaborators, C. (2019). THE CONCISE GUIDE TO PHARMACOLOGY 2019/20: Ion channels. British Journal of Pharmacology, 176(S1), S142-S228. doi:10.1111/bph.14749

Alexander, S. P. H., Roberts, R. E., Broughton, B. R. S., Sobey, C. G., George, C. H., Stanford, S. C., . . . Ahluwalia, A. (2018). Goals and practicalities of immunoblotting and immunohistochemistry: A guide for submission to the British Journal of Pharmacology. *British Journal of Pharmacology, 175*(3), 407-411. doi:10.1111/bph.14112

Becker, F., Reid, C. A., Hallmann, K., Tae, H. S., Phillips, A. M., Teodorescu, G., . . . Maljevic, S. (2017). Functional variants in HCN4 and CACNA1H may contribute to genetic generalized epilepsy. *Epilepsia Open, 2*(3), 334-342. doi:10.1002/epi4.12068

Benarroch, E. E. (2013). HCN channels: function and clinical implications. *Neurology, 80*(3), 304-310. doi:10.1212/WNL.0b013e31827dec42

Bender, R. A., & Baram, T. Z. (2008). Hyperpolarization activated cyclic-nucleotide gated (HCN) channels in developing neuronal networks. *Prog Neurobiol, 86*(3), 129-140. doi:10.1016/j.pneurobio.2008.09.007

Biel, M., Wahl-Schott, C., Michalakis, S., & Zong, X. (2009). Hyperpolarization-activated cation channels: from genes to function. *Physiol Rev, 89*(3), 847-885. doi:10.1152/physrev.00029.2008

Blumenfeld, H. (2005). Cellular and network mechanisms of spike-wave seizures. *Epilepsia, 46 Suppl 9*, 21-33. doi:10.1111/j.1528-1167.2005.00311.x

Bonzanni, M., DiFrancesco, J. C., Milanesi, R., Campostrini, G., Castellotti, B., Bucchi, A., . . . DiFrancesco, D. (2018). A novel de novo HCN1 loss-of-function mutation in genetic generalized epilepsy causing increased neuronal excitability. *Neurobiol Dis, 118*, 55-63. doi:10.1016/j.nbd.2018.06.012

Cain, S. M., Tyson, J. R., Jones, K. L., & Snutch, T. P. (2015). Thalamocortical neurons display suppressed burst-firing due to an enhanced Ih current in a genetic model of absence epilepsy. *Pflugers Arch, 467*(6), 1367-1382. doi:10.1007/s00424-014-1549-4

Campostrini, G., DiFrancesco, J. C., Castellotti, B., Milanesi, R., Gnecchi-Ruscone, T., Bonzanni, M., . . . DiFrancesco, D. (2018). A Loss-of-Function HCN4 Mutation Associated With Familial Benign Myoclonic Epilepsy in Infancy Causes Increased Neuronal Excitability. *Front Mol Neurosci, 11*, 269. doi:10.3389/fnmol.2018.00269

Chen, K., Aradi, I., Thon, N., Eghbal-Ahmadi, M., Baram, T. Z., & Soltesz, I. (2001). Persistently modified h-channels after complex febrile seizures convert the seizure-induced enhancement of inhibition to hyperexcitability. *Nat Med, 7*(3), 331-337. doi:10.1038/85480

Chiu, C., Reid, C. A., Tan, H. O., Davies, P. J., Single, F. N., Koukoulas, I., . . . Petrou, S. (2008). Developmental impact of a familial GABAA receptor epilepsy mutation. *Ann Neurol, 64*(3), 284-293. doi:10.1002/ana.21440

Chung, W. K., Shin, M., Jaramillo, T. C., Leibel, R. L., LeDuc, C. A., Fischer, S. G., . . . Chetkovich, D. M. (2009). Absence epilepsy in apathetic, a spontaneous mutant mouse lacking the h channel subunit, HCN2. *Neurobiol Dis, 33*(3), 499-508. doi:10.1016/j.nbd.2008.12.004

Colombi, I., Mahajani, S., Frega, M., Gasparini, L., & Chiappalone, M. (2013). Effects of antiepileptic drugs on hippocampal neurons coupled to micro-electrode arrays. *Front Neuroeng, 6*, 10. doi:10.3389/fneng.2013.00010

Curtis, M. J., Alexander, S., Cirino, G., Docherty, J. R., George, C. H., Giembycz, M. A., . . . Ahluwalia, A. (2018). Experimental design and analysis and their reporting II: updated and simplified guidance for authors and peer reviewers. *British Journal of Pharmacology, 175*(7), 987-993. doi:10.1111/bph.14153

David, F., Carcak, N., Furdan, S., Onat, F., Gould, T., Meszaros, A., . . . Crunelli, V. (2018). Suppression of Hyperpolarization-Activated Cyclic Nucleotide-Gated Channel Function in Thalamocortical Neurons Prevents Genetically Determined and Pharmacologically Induced Absence Seizures. *J Neurosci, 38*(30), 6615-6627. doi:10.1523/jneurosci.0896-17.2018

Del Lungo, M., Melchiorre, M., Guandalini, L., Sartiani, L., Mugelli, A., Koncz, I., . . . Cerbai, E. (2012). Novel blockers of hyperpolarization-activated current with isoform selectivity in recombinant cells and native tissue. *Br J Pharmacol, 166*(2), 602-616. doi:10.1111/j.1476-5381.2011.01782.x

Dibbens, L. M., Reid, C. A., Hodgson, B., Thomas, E. A., Phillips, A. M., Gazina, E., . . . Petrou, S. (2010). Augmented currents of an HCN2 variant in patients with febrile seizure syndromes. *Ann Neurol, 67*(4), 542-546. doi:10.1002/ana.21909

DiFrancesco, J. C., & DiFrancesco, D. (2015). Dysfunctional HCN ion channels in neurological diseases. *Front Cell Neurosci, 6*, 174. doi:10.3389/fncel.2015.00071

Gazina, E. V., Morrisroe, E., Mendis, G. D. C., Michalska, A. E., Chen, J., Nefzger, C. M., . . . Petrou, S. (2018). Method of derivation and differentiation of mouse embryonic stem cells generating synchronous neuronal networks. *Journal of Neuroscience Methods, 293*, 53-58. doi:https://doi.org/10.1016/j.jneumeth.2017.08.018

Hammelmann, V., Stieglitz, M. S., Hulle, H., Le Meur, K., Kass, J., Brummer, M., . . . Biel, M. (2019). Abolishing cAMP sensitivity in HCN2 pacemaker channels induces generalized seizures. *JCI Insight, 4*(9). doi:10.1172/jci.insight.126418

Harding, S. D., Sharman, J. L., Faccenda, E., Southan, C., Pawson, A. J., Ireland, S., . . . NC-IUPHAR. (2017). The IUPHAR/BPS Guide to PHARMACOLOGY in 2018: updates and expansion to encompass the new guide to IMMUNOPHARMACOLOGY. Nucleic Acids Research, 46(D1), D1091-D1106. doi:10.1093/nar/gkx1121

Heffner, C. (2011). Intraperitoneal Injection of Tamoxifen for Inducible Cre-Driver Lines. Retrieved from https://www.jax.org/research-and-faculty/resources/cre-repository/tamoxifen

Heimer-McGinn, V., & Young, P. (2011). Efficient inducible Pan-neuronal cre-mediated recombination in SLICK-H transgenic mice. *Genesis, 49*(12), 942-949. doi:10.1002/dvg.20777

Herrmann, S., Hofmann, F., Stieber, J., & Ludwig, A. (2012). HCN channels in the heart: lessons from mouse mutants. *Br J Pharmacol, 166*(2), 501-509. doi:10.1111/j.1476-5381.2011.01798.x

Herrmann, S., Stieber, J., Stockl, G., Hofmann, F., & Ludwig, A. (2007). HCN4 provides a 'depolarization reserve' and is not required for heart rate acceleration in mice. *EMBO J, 26*(21), 4423-4432. doi:10.1038/sj.emboj.7601868

Kilkenny, C., Browne, W. J., Cuthill, I. C., Emerson, M., & Altman, D. G. (2010). Improving Bioscience Research Reporting: The ARRIVE Guidelines for Reporting Animal Research. *PLOS Biology, 8*(6), e1000412. doi:10.1371/journal.pbio.1000412

Kitayama, M., Miyata, H., Yano, M., Saito, N., Matsuda, Y., Yamauchi, T., & Kogure, S. (2003). Ih blockers have a potential of antiepileptic effects. *Epilepsia, 44*(1), 20-24.

Koruth, J. S., Lala, A., Pinney, S., Reddy, V. Y., & Dukkipati, S. R. (2017). The Clinical Use of Ivabradine. *J Am Coll Cardiol, 70*(14), 1777-1784. doi:10.1016/j.jacc.2017.08.038

Laemmli, U. K. (1970). Cleavage of Structural Proteins during the Assembly of the Head of Bacteriophage T4. *Nature, 227*(5259), 680-685. doi:10.1038/227680a0

Loscher, W. (2011). Critical review of current animal models of seizures and epilepsy used in the discovery and development of new antiepileptic drugs. *Seizure, 20*(5), 359-368. doi:10.1016/j.seizure.2011.01.003

Ludwig, A., Budde, T., Stieber, J., Moosmang, S., Wahl, C., Holthoff, K., . . . Hofmann, F. (2003). Absence epilepsy and sinus dysrhythmia in mice lacking the pacemaker channel HCN2. *EMBO J, 22*(2), 216-224. doi:10.1093/emboj/cdg032

Luszczki, J. J., Prystupa, A., Andres-Mach, M., Marzeda, E., & Florek-Luszczki, M. (2013). Ivabradine (a hyperpolarization activated cyclic nucleotide-gated channel blocker) elevates the threshold for maximal electroshock-induced tonic seizures in mice. *Pharmacol Rep, 65*(5), 1407-1414.

Marini, C., Porro, A., Rastetter, A., Dalle, C., Rivolta, I., Bauer, D., . . . Depienne, C. (2018). HCN1 mutation spectrum: from neonatal epileptic encephalopathy to benign generalized epilepsy and beyond. *Brain, 141*(11), 3160-3178. doi:10.1093/brain/awy263

Matsuda, Y., Saito, N., Yamamoto, K., Niitsu, T., & Kogure, S. (2008). Effects of the Ih blockers CsCl and ZD7288 on inherited epilepsy in Mongolian gerbils. *Exp Anim, 57*(4), 377-384.

McSweeney, K. M., Gussow, A. B., Bradrick, S. S., Dugger, S. A., Gelfman, S., Wang, Q., . . . Goldstein, D. B. (2016). Inhibition of microRNA 128 promotes excitability of cultured cortical neuronal networks. *Genome research, 26*(10), 1411-1416. doi:10.1101/gr.199828.115

Mendis, G. D. C., Berecki, G., Morrisroe, E., Pachernegg, S., Li, M., Varney, M., . . . Petrou, S. (2019). Discovering the pharmacodynamics of conolidine and cannabidiol using a cultured neuronal network based workflow. *Scientific Reports*, 9(1), 121. doi:10.1038/s41598-018-37138-w

Mendis, G. D. C., Morrisroe, E., Petrou, S., & Halgamuge, S. K. (2016). Use of adaptive network burst detection methods for multielectrode array data and the generation of artificial spike patterns for method evaluation. *Journal of Neural Engineering, 13*(2), 026009. doi:10.1088/1741-2560/13/2/026009

Moosmang, S., Biel, M., Hofmann, F., & Ludwig, A. (1999). Differential distribution of four hyperpolarization-activated cation channels in mouse brain. *Biol Chem, 380*(7-8), 975-980. doi:10.1515/BC.1999.121

Nava, C., Dalle, C., Rastetter, A., Striano, P., de Kovel, C. G., Nabbout, R., . . . Depienne, C. (2014). De novo mutations in HCN1 cause early infantile epileptic encephalopathy. *Nat Genet, 46*(6), 640-645. doi:10.1038/ng.2952

Nicolazzo, J. A., Steuten, J. A., Charman, S. A., Taylor, N., Davies, P. J., & Petrou, S. (2010). Brain uptake of diazepam and phenytoin in a genetic animal model of absence epilepsy. *Clin Exp Pharmacol Physiol, 37*(5-6), 647-649. doi:10.1111/j.1440-1681.2010.05362.x

Oyrer, J., Bleakley, L. E., Richards, K. L., Maljevic, S., Phillips, A. M., Petrou, S., . . . Reid, C. A. (2019). Using a Multiplex Nucleic Acid in situ Hybridization Technique to Determine HCN4 mRNA Expression in the Adult Rodent Brain. *Front Mol Neurosci, 12*, 211-211. doi:10.3389/fnmol.2019.00211

Pape, H. C. (1996). Queer current and pacemaker: the hyperpolarization-activated cation current in neurons. *Annu Rev Physiol, 58*, 299-327. doi:10.1146/annurev.ph.58.030196.001503

Paz, J. T., Davidson, T. J., Frechette, E. S., Delord, B., Parada, I., Peng, K., . . . Huguenard, J. R. (2013). Closed-loop optogenetic control of thalamus as a tool for interrupting seizures after cortical injury. *Nat Neurosci, 16*(1), 64-70. doi:10.1038/nn.3269

Pfaffl, M. W. (2001). A new mathematical model for relative quantification in real-time RT-PCR. *Nucleic Acids Res, 29*(9), e45.

Phillips, A. M., Kim, T., Vargas, E., Petrou, S., & Reid, C. A. (2014). Spike-and-wave discharge mediated reduction in hippocampal HCN1 channel function associates with learning deficits in a genetic mouse model of epilepsy. *Neurobiol Dis, 64*, 30-35. doi:https://doi.org/10.1016/j.nbd.2013.12.007

Powell, K. L., Ng, C., O'Brien, T. J., Xu, S. H., Williams, D. A., Foote, S. J., & Reid, C. A. (2008). Decreases in HCN mRNA expression in the hippocampus after kindling and status epilepticus in adult rats. *Epilepsia, 49*(10), 1686-1695. doi:10.1111/j.1528-1167.2008.01593.x

Reid, C. A., Kim, T., Phillips, A. M., Low, J., Berkovic, S. F., Luscher, B., & Petrou, S. (2013). Multiple molecular mechanisms for a single GABA A mutation in epilepsy. *Neurology, 80*(11), 1003. Retrieved from http://n.neurology.org/content/80/11/1003.abstract

Reid, C. A., Phillips, A. M., & Petrou, S. (2012). HCN channelopathies: pathophysiology in genetic epilepsy and therapeutic implications. *Br J Pharmacol, 165*(1), 49-56. doi:10.1111/j.1476-5381.2011.01507.x

Robinson, R. B., & Siegelbaum, S. A. (2003). Hyperpolarization-activated cation currents: from molecules to physiological function. *Annu Rev Physiol, 65*, 453-480. doi:10.1146/annurev.physiol.65.092101.142734

Romanelli, M. N., Del Lungo, M., Guandalini, L., Zobeiri, M., Gyokeres, A., Arpadffy-Lovas, T., . . . Cerbai, E. (2019). EC18 as a Tool To Understand the Role of HCN4 Channels in Mediating Hyperpolarization-Activated Current in Tissues. *ACS Med Chem Lett, 10*(4), 584-589. doi:10.1021/acsmedchemlett.8b00587

Romanelli, M. N., Sartiani, L., Masi, A., Mannaioni, G., Manetti, D., Mugelli, A., & Cerbai, E. (2016). HCN Channels Modulators: The Need for Selectivity. *Current Topics in Medicinal Chemistry, 16*(16), 1764-1791. doi:10.2174/1568026616999160315130832

Santoro, B., Chen, S., Luthi, A., Pavlidis, P., Shumyatsky, G. P., Tibbs, G. R., & Siegelbaum, S. A. (2000). Molecular and functional heterogeneity of hyperpolarization-activated pacemaker channels in the mouse CNS. *J Neurosci, 20*(14), 5264-5275.

Santoro, B., Lee, J. Y., Englot, D. J., Gildersleeve, S., Piskorowski, R. A., Siegelbaum, S. A., . . . Blumenfeld, H. (2010). Increased seizure severity and seizure-related death in mice lacking HCN1 channels. *Epilepsia, 51*(8), 1624-1627. doi:10.1111/j.1528-1167.2010.02554.x

Sartiani, L., Mannaioni, G., Masi, A., Novella Romanelli, M., & Cerbai, E. (2017). The Hyperpolarization-Activated Cyclic Nucleotide–Gated Channels: from Biophysics to Pharmacology of a Unique Family of Ion Channels. *Pharmacological Reviews, 69*(4), 354-395. doi:10.1124/pr.117.014035

Savelieva, I., & Camm, A. J. (2006). Novel I_f Current Inhibitor Ivabradine: Safety Considerations. *Advances in Cardiology*, 43, 79-96. doi:10.1159/000095430

Savelieva, I., & Camm, A. J. (2008). I_f inhibition with ivabradine: electrophysiological effects and safety. *Drug Safety*, 31(2), 95-107. doi:10.2165/00002018-200831020-00001

Schneider, C. A., Rasband, W. S., & Eliceiri, K. W. (2012). NIH Image to ImageJ: 25 years of image analysis. *Nat Methods, 9*(7), 671-675.

Stieber, J., Herrmann, S., Feil, S., Loster, J., Feil, R., Biel, M., . . . Ludwig, A. (2003). The hyperpolarization-activated channel HCN4 is required for the generation of pacemaker action potentials in the embryonic heart. *Proc Natl Acad Sci U S A, 100*(25), 15235-15240. doi:10.1073/pnas.2434235100

Strauss, U., Kole, M. H., Brauer, A. U., Pahnke, J., Bajorat, R., Rolfs, A., . . . Deisz, R. A. (2004). An impaired neocortical Ih is associated with enhanced excitability and absence epilepsy. *Eur J Neurosci, 19*(11), 3048-3058. doi:10.1111/j.0953-816X.2004.03392.x

Surges, R., Kukley, M., Brewster, A., Ruschenschmidt, C., Schramm, J., Baram, T. Z., . . . Dietrich, D. (2012). Hyperpolarization-activated cation current Ih of dentate gyrus granule cells is upregulated in human and rat temporal lobe epilepsy. *Biochem Biophys Res Commun, 420*(1), 156-160. doi:10.1016/j.bbrc.2012.02.133

Tae, H. S., Smith, K. M., Phillips, A. M., Boyle, K. A., Li, M., Forster, I. C., . . . Reid, C. A. (2017). Gabapentin Modulates HCN4 Channel Voltage-Dependence. *Front Pharmacol, 8*, 554. doi:10.3389/fphar.2017.00554

Yuen, E. S., & Troconiz, I. F. (2015). Can pentylenetetrazole and maximal electroshock rodent seizure models quantitatively predict antiepileptic efficacy in humans? *Seizure, 24*, 21-27. doi:10.1016/j.seizure.2014.11.006

Zobeiri, M., Chaudhary, R., Blaich, A., Rottmann, M., Herrmann, S., Meuth, P., . . . Ludwig, A. (2019). The Hyperpolarization-Activated HCN4 Channel is Important for Proper Maintenance of Oscillatory Activity in the Thalamocortical System. *Cereb Cortex, 29*(5), 2291-2304. doi:10.1093/cercor/bhz047

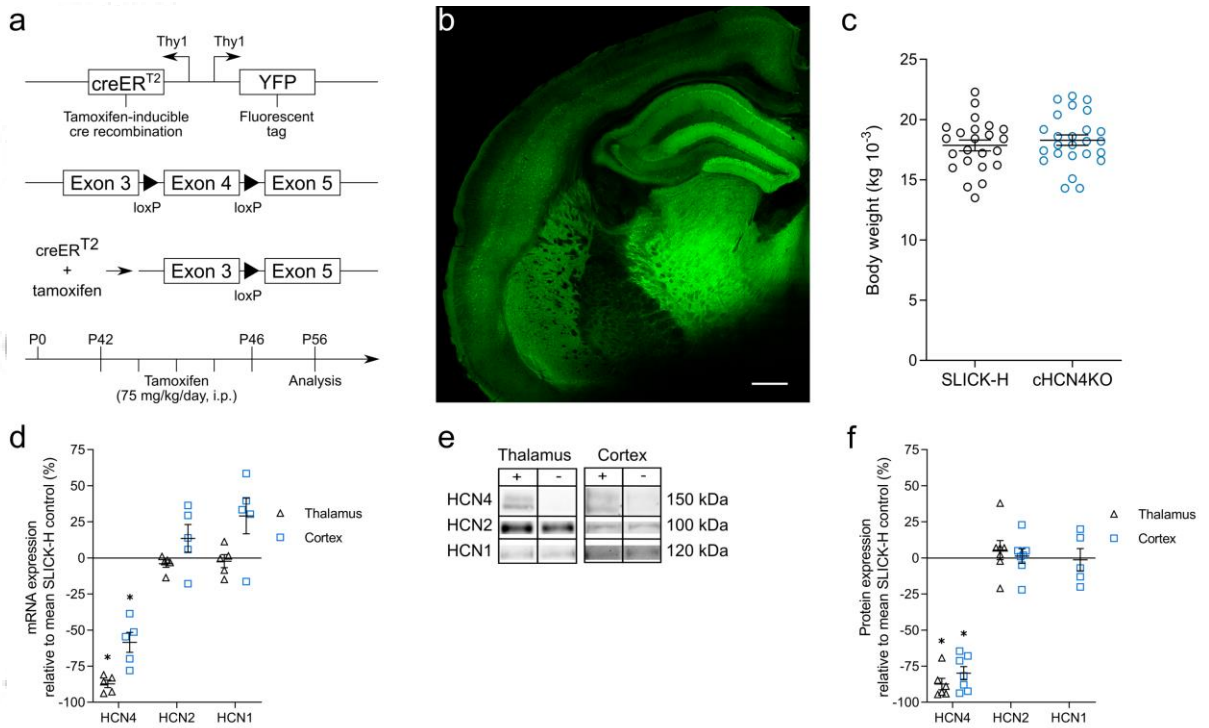

Figure 1. Characterization of the cHCN4KO mouse model. (a) Cartoon of the SLICK-H transgene, the *HCN4* exon deleted using the Cre/loxP system after the administration of tamoxifen, and the experimental timeline used. (b) Brain section showing typical Thy1 promoter eYFP brain expression in SLICK-H mice (repeated in n=3 mice, Scale bar=600µm). (c) Body weight of SLICK-H and cHCN4KO mice 10 days after tamoxifen treatment. Data shown are individual values and mean ± S.E.M. (SLICK-H n=23, cHCN4KO n=25). (d) HCN mRNA expression in the cHCN4KO brain (n=5) relative to the mean of the SLICK-H control (n=5). GAPDH was used as a reference gene for normalisation, and each run was analysed separately. HCN4 mRNA levels were reduced in the cHCN4KO mouse relative to SLICK-H controls. The expression of HCN1 and HCN2 mRNA in thalamus and cortex tissue was unchanged. (e) Typical examples of protein expression on Western blots of HCN isoforms (100mg of total protein/lane) in cHCN4KO (-) and SLICK-H (+) mouse tissue. Depending on the brain region and the HCN isoform being analysed the exposure time ranged between 5 and 400s. HCN1 in thalamus was at background levels. (f) HCN protein expression in the cHCN4KO brain relative to the mean of the SLICK-H control. Blots were analysed separately by ImageJ. (HCN1 protein expression levels of thalamus-enriched tissue were too low to analyse). (Thalamus n=6, Cortex n=7). Exploratory Western blots of other isoforms showed no differences compared to SLICK-H controls (Fig. S1). F-test analysis showed no significant differences in variance. No reduction in HCN4 expression was seen in one mouse. As this was outside confidence levels it was excluded from analysis. Data expressed as individual values and mean ± S.E.M. *p<0.05 vs. SLICK-H mean via Wilcoxon matched pairs signed-rank test.

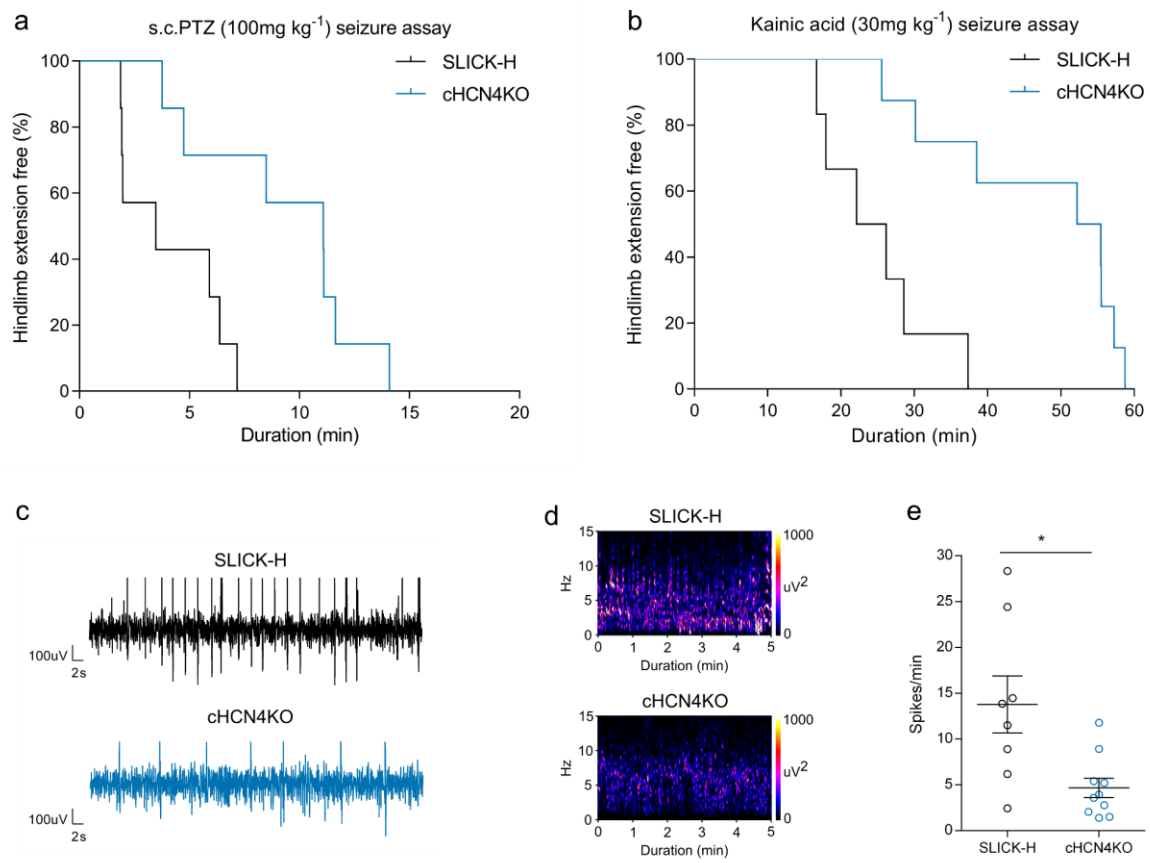

Figure 2. Brain-specific HCN4 knockout reduces seizure susceptibility and ECoG activity. (a) s.c.PTZ (100mg kg^{-1}) increased hindlimb extension seizure latency. $p<0.05$ vs. SLICK-H via log-rank (Mantel-Cox) test. (SLICK-H n=7, cHCN4KO n=7). (b) Kainic acid (30mg kg^{-1}) increased hindlimb extension seizure latency. $p<0.05$ vs. SLICK-H via log-rank (Mantel-Cox) test. (SLICK-H n=6, cHCN4KO n=8). Mice that did not have any seizures were excluded from analysis (SLICK-H n=2, cHCN4KO n=1). (c) Electrocorticography (ECoG) recording showing the effect of brain-specific HCN4 knockout on low-dose PTZ-induced spiking over a period of 60s. (d) ECoG power spectra showing the effect of brain-specific HCN4 knockout after the administration of low-dose PTZ (60mg kg^{-1}) over a five minute period. (e) Rate of PTZ-induced spiking over a 10 minute period after low-dose PTZ administration. F-test analysis showed significant differences in variance (SLICK-H n=8, cHCN4KO n=10). Data expressed as individual values and mean ± S.E.M., *$p<0.05$ vs. SLICK-H via two-tailed Mann-Whitney U test.

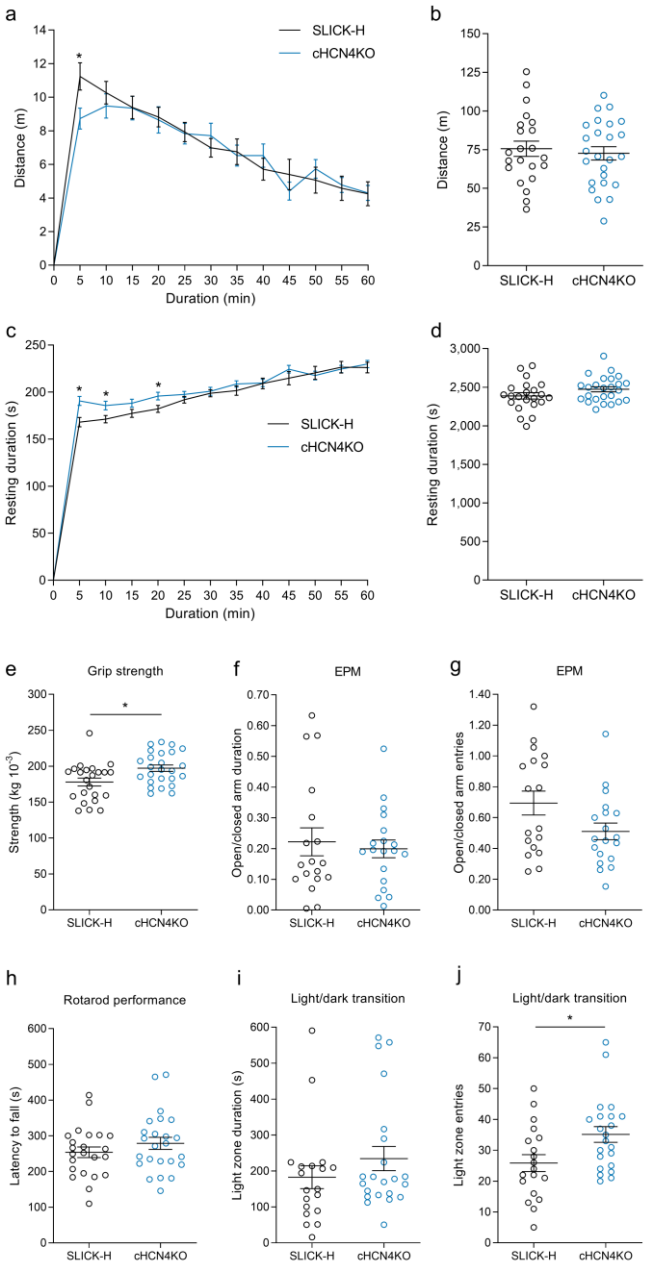

Figure 3. Behavioural characterisation of the SLICK-H and cHCN4KO mouse model. (a, b) Distance travelled (m) in the open field locomotor cell over a 60 minute period (SLICK-H n=22, cHCN4KO n=25). (c, d) Resting duration (s) in the open field locomotor cell over a 60 minute period (SLICK-H n=22, cHCN4KO n=25). (e) Maximum force (kg 10^{-3}) measured during the grip strength test (SLICK-H n=23, cHCN4KO n=25). (f, g) Elevated plus maze (EPM) open arm duration (f), and entries (g) relative to the closed arm (SLICK-H n=18, cHCN4KO n=19). (h) Maximum latency to fall (s) measured during the rotarod performance test (SLICK-H n=23, cHCN4KO n=25). (i, j) Light zone duration (s) (i), and entries (j) during the light/dark transition test (SLICK-H n=19, cHCN4KO n=22). F-test analysis showed no significant differences in variance. Data expressed as individual values and mean ± S.E.M., *p<0.05 vs. SLICK-H via Student's two-tailed unpaired t-test. A two factor ANOVA test found that there were no sex differences in any behavioural measures.

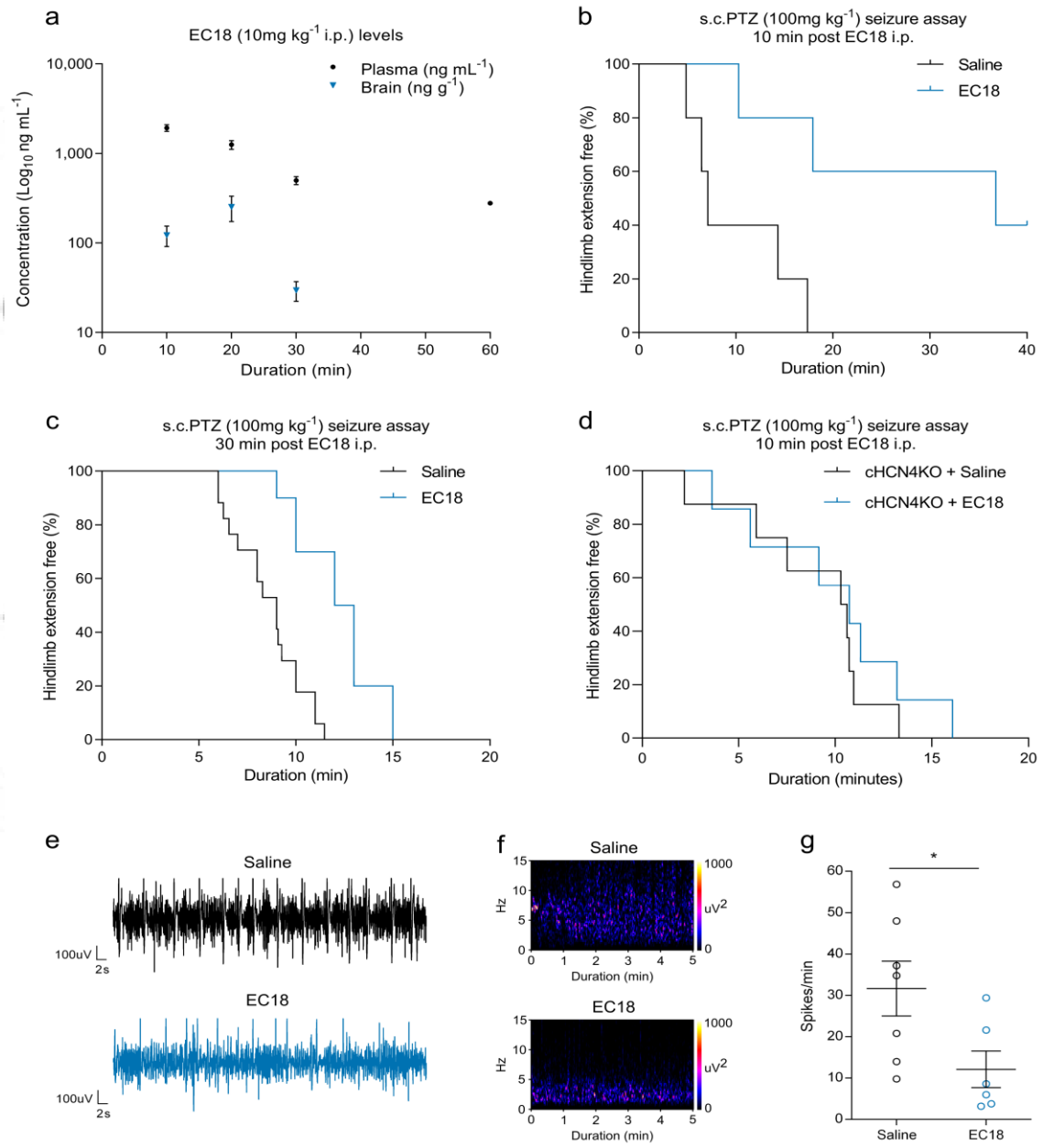

Figure 4. Effect of the HCN4 channel blocker EC18 on seizure susceptibility and ECoG activity. (a) Plasma and brain concentrations of EC18 (10mg kg^{-1}) following an i.p. injection. Data expressed as individual values and mean ± SD on a Log_{10} scale. (b) s.c.PTZ induced hindlimb extension seizure latency 10 minutes post EC18 (10mg kg^{-1}, i.p.) injection in C57BL/6J mice. $p<0.05$ vs. Saline via log-rank (Mantel-Cox) test. (Saline n=5, EC18 n=5) (c) s.c.PTZ induced hindlimb extension seizure latency 30 minutes post EC18 (10mg kg^{-1}, i.p.) injection in C57BL/6J mice. $p<0.05$ vs. Saline via log-rank (Mantel-Cox) test. (Saline n=17, EC18 n=10). (d) Effect of EC18 (10mg kg^{-1}, i.p.) on s.c.PTZ induced hindlimb extension seizure latency of the cHCN4KO mouse 10 minutes post injection. $p=0.670$ vs. cHCN4KO + Saline via log-rank (Mantel-Cox) test. (cHCN4KO + Saline n=8, cHCN4KO + EC18 n=7). (e) Electrocorticography (ECoG) recording showing the effect of EC18 on low-dose 60mg kg^{-1} PTZ-induced spiking over a period of 60s. (f) ECoG power spectra showing the effect of EC18 after the administration of low-dose PTZ (60mg kg^{-1}) over a five minute period. (g) Rate of low-dose 60mg kg^{-1} PTZ-induced spiking over a 10 minute period after PTZ administration in C57BL/6J mice. F-test analysis showed no significant differences in variance (Saline n=7, EC18 n=6). Data expressed as individual values and mean ± S.E.M., *$p<0.05$ vs. Saline via Student's two-tailed unpaired t-test.

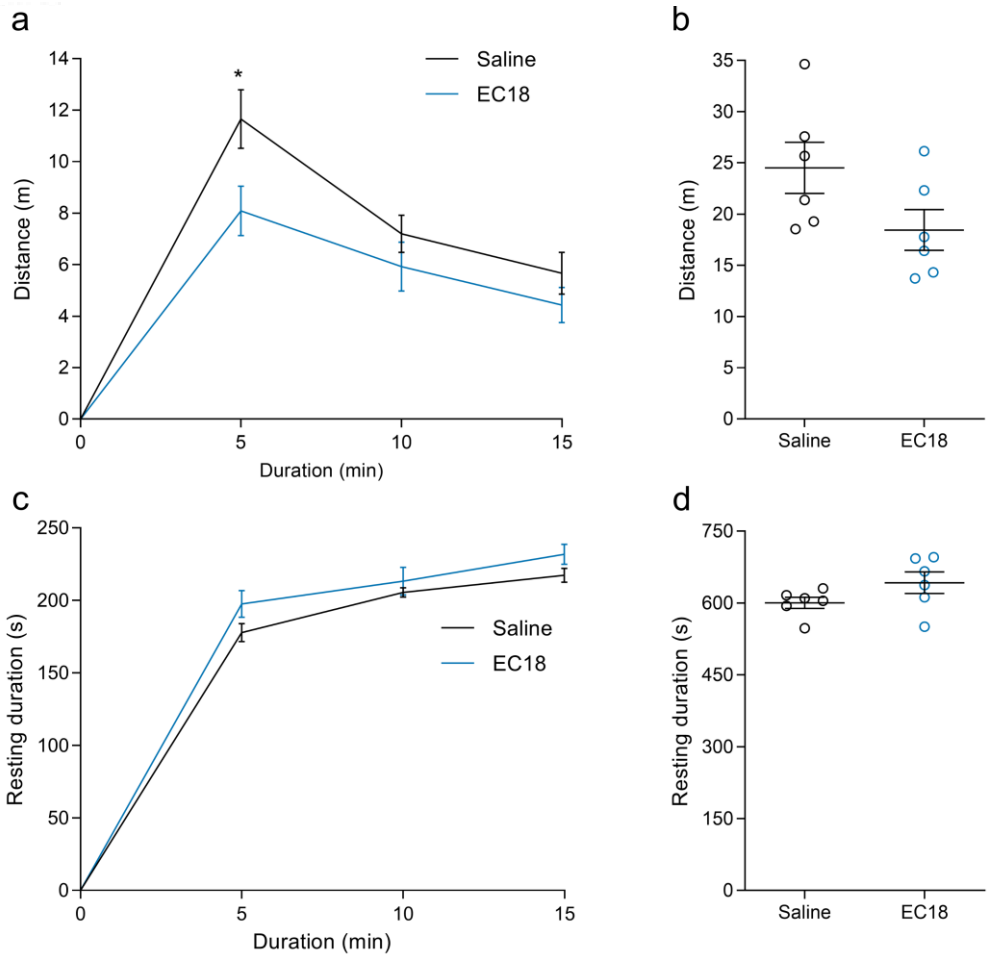

Figure 5. Effect of EC18 (10mg kg^{-1} i.p.) on locomotor activity. (a, b) Distance travelled (m) 30 minutes post injection of EC18 in the open field locomotor cell over a 15 minute period (*p<0.05, Saline n=6, EC18 n=6). (c, d) Resting duration (s) 30 minutes post injection of EC18 in the open field locomotor cell over a 15 minute period (Saline n=6, EC18 n=6). F-test analysis showed no significant differences in variance. Data expressed as individual values (b, d) and mean ± S.E.M., *p<0.05 vs. Saline via Student's two-tailed unpaired t-test.

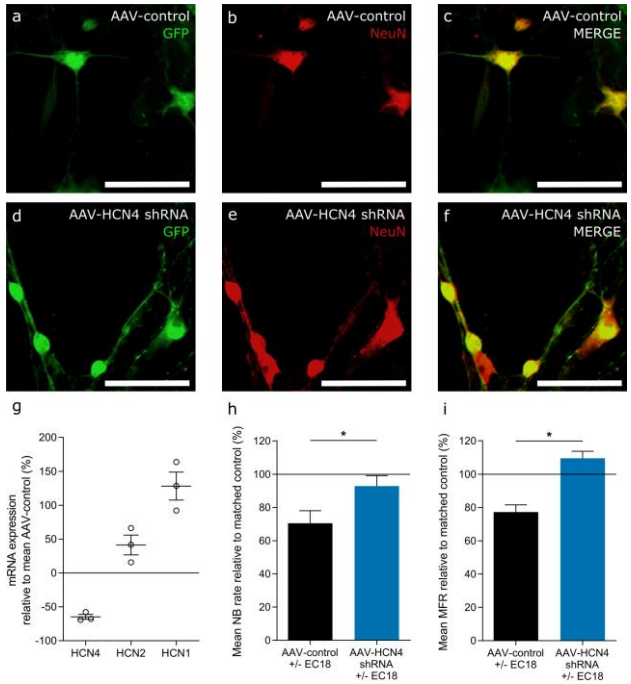

Figure 6. EC18 reduces cultured neuronal network excitability in an HCN4 channel dependent manner. (a-f) GFP and NeuN expression in neurons infected with (a-c) AAV-control or (d-f) AAV-HCN4 shRNA (Scale bar=50µm). (g) HCN mRNA expression of AAV-HCN4 shRNA infected culture relative to AAV-control in three independent experiments involving cells pooled from 8-10 neonatal mice. (h) Relative change in network burst (NB) rate (Hz) and (i) mean firing rate (MFR) of AAV-control and AAV-HCN4 shRNA infected cortical pooled cells from 8-12 neonatal mice after 10µM EC18 treatment. Data expressed as mean ± S.E.M., *p<0.05 vs. AAV-control via Wilcoxon matched pairs signed-rank test (AAV-control +/- EC18 n=12 wells, AAV-HCN4 shRNA +/- EC18 n=11 wells). NB = network burst and MFR= mean firing rate.